

1

NETWORK MODEL

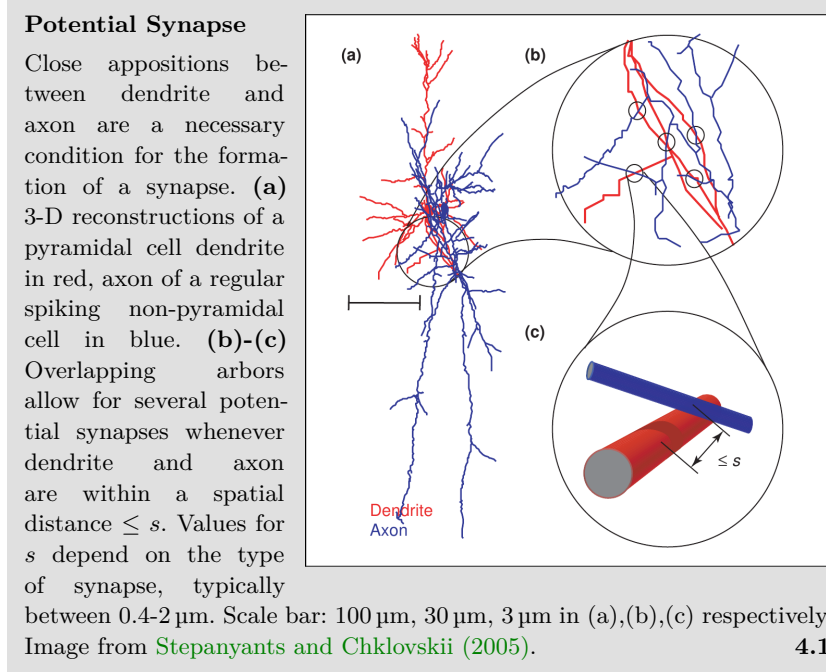
Motivated by anisotropic characteristics in connectivity in local cortical circuits found in the rat's brain, a network model with anisotropic tissue geometry is developed. Employing both a graph theoretic definition and a numerical implementation, distance-dependent connectivity present in the model is exposed. The introduction of a rewiring algorithm and quantitative anisotropy measure lays the foundation for the analysis of structural aspects of the anisotropic network model in Chapter ??.

1.1 INTRODUCTION

This chapter introduces the central object of this study, the *anisotropic network model*. Reviewing connectivity in local cortical circuits in Section 1.2, we find evidence of anisotropy in connectivity that we try capture in the network model introduced in Section 1.3. Forcing this specific geometry in network however, causes for . For our ana

1.2 ANISOTROPY IN NEURAL CONNECTIVITY

Neurogeometry addresses the problem of inferring synaptic connectivity from the geometric shapes of axon and dendrites. A fundamental concept in this field is that of a *potential synapse* (Stepanyants et al. 2002). Defined as the potential axonal-dendritic connection of two neurons, present whenever the axon of one neuron is within a spatial distance s of the dendrite of the other, it is a necessary, although not sufficient, condition for the formation of a synaptic connection (Figure 1.1). The existence of such close appositions solely depends on dendritic and axonal anatomy; identification of defining morphological characteristics in both axon and dendrite would therefore allow for a model of local network connectivity, assuming for example that a certain ratio r of potential synapses turn into active contacts independently. It is the hope that such a model, motivated from the geometry of a neuron's functional compartments, not only displays inherent patterns of connectivity similar to what has been observed in biological networks, but also proofs itself as a testing ground for how this connectivity may affect network dynamics.



high variability in
axonal
morphology

Finding stereotypical anatomical characteristics however is difficult, as axonal morphology is, in general, highly diverse (Debanne 2004). Across different species, distinct regions in the central nervous system and different neuron types, axons display a wide variety of shapes characterized by morphometric parameters such as total length, branching complexity and axonal extent (Ropireddy et al. 2011). Typical exam-

ples of distinct morphology include the T-shaped axons of cerebellar granule cells branching only at a singular point (Ramon and Cajal 1911), and axons of hippocampal CA3 pyramidal cells, which, in stark contrast, may feature up to 40 branches resulting in a total length of axon collaterals of up to 12 mm (Ishizuka et al. 1990).

It is therefore imperative to confine this analysis to a specific brain region and neuron type. In this study, we set the focus on circuits of pyramidal cells in the mammalian cortex. More specifically, local circuits of thick tufted layer V pyramidal neurons in the rat's somatosensory cortex have been the target of advanced experimentation (Song et al. 2005; Perin et al. 2011; Romand et al. 2011; Ramaswamy et al. 2012), and will serve as a benchmark for results in neural morphology and network connectivity in this report.

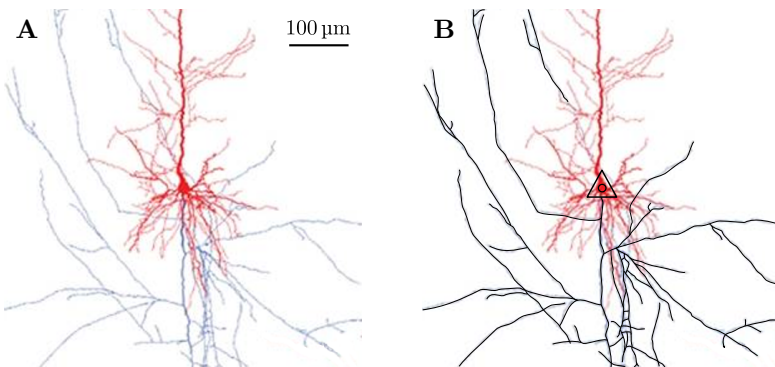


Figure 1.2: Tracing axonal branching of a pyramidal cell In a 3-D model reconstructed from biocytin-labeled thick-tufted layer V pyramidal cells in the somatosensory cortex of postnatal (day 14) Wistar rats, Romand et al. (2011) depict dendritic compartments in red, axonal compartments in blue. **A)** A 600 μm window centered on the soma of the pyramidal cell shows the main stem of the cell's axon projecting downwards in a straight line, collaterals branching at various angles. **B)** Using image manipulation software, axon morphology was manually traced and is emphasized in black.

Axonal morphology of pyramidal cells in the cerebral cortex is well described. From the soma the single main stem of the axon originates and projects downwards, describing a trajectory closely resembling a straight line (Braitenberg and Schüz 1998). At arbitrary points along this path, collaterals branch off at various angles and constitute themselves linear paths until they further ramify or terminate. Displaying a high degree of ramification, axonal trees of cortical pyramidal cells build, in general, complex structures (Petersen et al. 2003; Ramaswamy et al. 2012). Cortical slice experiments analyzing neural anatomy are typically constrained by a slice thickness of 300 μm . On this scale, 3-D reconstruction from labeled thick tufted layer V pyramidal cells reveals

cortical axons
form straight lines,
arborize profusely

characteristic morphology of the axonal tree (Figure 1.2). The downwards projecting, straight axon branches at several points, forming collateral branches that travel in linear path as well.

In a statistical view, this characteristic axonal morphology results in high axon branch densities along the main stem, whereas distant regions display a relatively low density (Figure 1.3). Specifically, axon collaterals do not cluster around the soma but align with the main stem's projection. As presence of an axonal branch constitutes a necessary condition for a potential synapse, a higher concentration of potential and, subsequently, realized synapses is expected in regions of high branch density. For a coherent picture of local connectivity profiles, however, dendritic morphology needs to be considered as well.

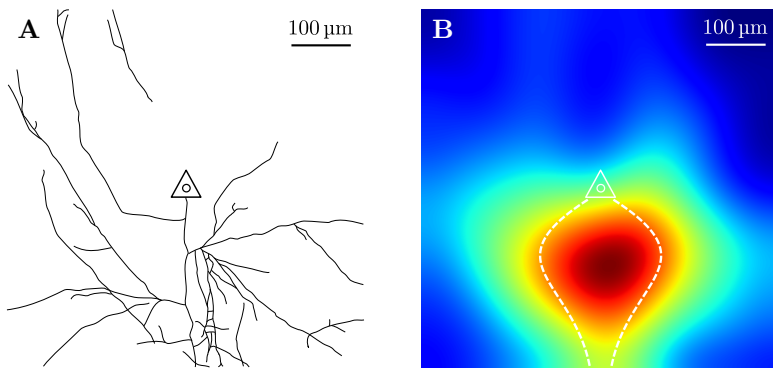


Figure 1.3: Illustrating axonal branch density In a sample of 5 reconstructions from thick-tufted layer V pyramidal cells (Romand et al. 2011), tracing axonal morphology illustrates characteristic branch density along the axon's main stem. **A)** Example of extracted axonal tree. Outline manually traced using image manipulation software. Soma indicated by triangle. Original data from Romand et al. (2011). **B)** Overlaying 5 axonal trees extracted as in A), applying a Gaussian filter and displaying high axon densities in warm colors, illustrates the characteristic higher branch densities along the axon's main stem.

basal dendrites dominate local connectivity

Dendritic anatomy of cortical pyramidal cells is inherently bipartite. From the soma several *basal dendrites* emerge and extend into arbitrary directions, branching profusely until they terminate. The single *apical dendrite* emerges from the apex of the pyramidal cell and ascends in a linear trajectory, forming occasional collateral branches until finally terminating into the apical tuft, where the dendrite branches several times to form a tree like structure (Feldman 1984). On the scale of typical cortical slice thickness, however, the apical dendrite is cut off and the basal dendrite dominates the dendritic morphology and potential of dendritic-axonal connections (Figure 1.4). The radial extension of dendritic branches results in a high concentration of dendritic branches

around the soma, much in the contrast to the findings of axonal branch densities before.

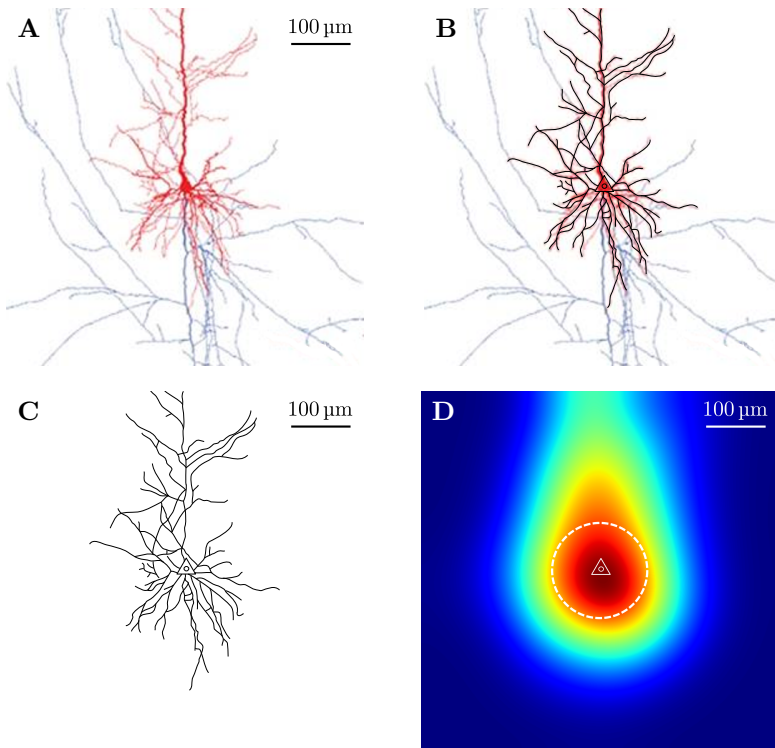


Figure 1.4: Dendritic morphology and branch density Using neuronal morphology of thick-tufted layer V pyramidal cells recorded by Romand et al. (2011), dendritic anatomy is traced and combined to illustrate high branch density around the soma. **A)** In a 600 μm window centered on the soma, basal dendrites (red) are visible extending around the soma. The ascending thick apical dendrite (red) is cut off and apical tuft is not shown. **B)-C)** Manual tracing of dendritic outlines in five samples (one shown), allows for clearer identification of stereotypical morphology and later analysis. **D)** Combining 5 dendritic outlines as shown in C) and subsequent Gaussian filtering reveals the relatively high dendritic branch density around the soma.

Combining the above results of dendritic and axonal branch densities in the light of neurogeometry, a clear concept of anisotropy of neural connectivity emerges. As dendritic branches of potential post-synaptic targets extend radially from the soma and do not display a preferred direction, target neurons for outgoing synaptic contacts originating from a single pyramidal cell, cluster around the downwards projecting axon (Figure 1.5). In their in-depth study, Stepanyants and Chklovskii (2005) confirm the overrepresentation of potential synapses along the axon for pyramidal cells. Consistent with the notion that stereotypical morphology of pyramidal cells is intrinsic to the local network's connectivity

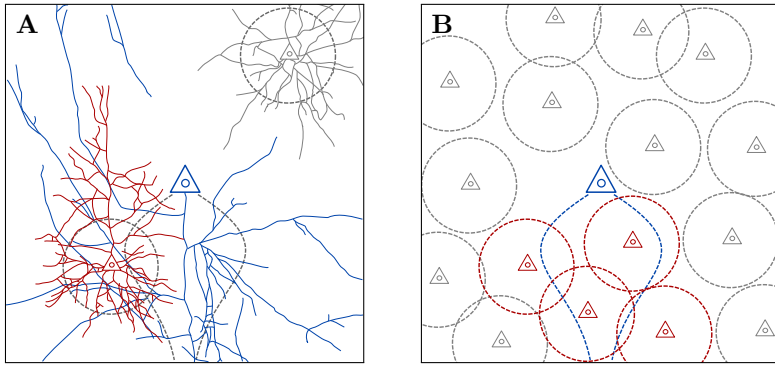


Figure 1.5: Connected neurons of a single pyramidal cell align with axonal projection Reducing the full axonal (blue, cf. Figure 1.2) and dendritic trees (red, gray, cf. Figure 1.4) as shown for two neurons in A) to their stereotypical axonal (blue) and dendritic profiles (red, gray) in B), demonstrates how connected neurons (red) tend to cluster around the pre-synaptic axon's profile, as spatial closeness constitutes a necessary condition for the formation of contacts. Unconnected neurons (gray) are found distant from the axon's projection, but not necessarily distant from the soma.

profile, they also find that anisotropy of this degree is *not* present in spiny stellate neurons located in lower-layer-4.

1.3 ANISOTROPIC GEOMETRIC NETWORK MODEL

Taking up the concept of anisotropy in neural connectivity introduced in the last section, we propose here, as basis for this study, a simple geometric network model featuring anisotropic connectivity. Constructing such a model, we're challenged with resembling the anisotropic aspects outlined last section as closely as possible, while at the same time basing the model on simple and abstract relations to allow for an analytical study of such anisotropic networks.

With this in mind, we propose the following model: On a square surface of side length s , a number of N point neurons are randomly, uniformly distributed. Connected neighbors are then calculated for each neuron separately and independently, by determining the randomly, uniformly distributed direction of the neuron's single axon. In this direction the axon traverses over the surface describing a straight path, terminating only when an edge of the surface is reached. Directed contacts are made with every neuron that is within a width $w(x)$ of the axon's trajectory, where in general w depends on the axon length x at this point (Figure 1.6).

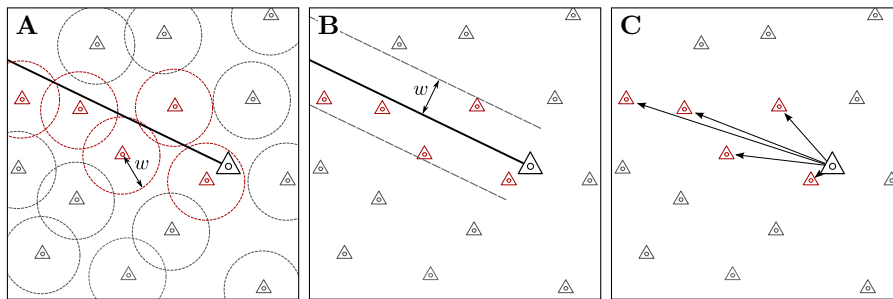


Figure 1.6: Anisotropic geometric network model and interpretations of width parameter w Illustrating the process of finding connections for one neuron (large triangle, black), the axon describes a linear trajectory in an arbitrary direction and until terminating on the surface's edge. Target neurons (red) are encountered along the path within a (here constant) distance w , which is in **A**) interpreted as a dendritic radius or, equivalently, in **B**) as a “bandwidth” of the axon. Connections to the encountered targets are then established as projections in **C**), consistent with the directed nature of synapses in biological networks (cf. Chapter ??).

The implementation of arbitrary axonal orientation is crucial to the model. Although cortical axons are described as consistently projecting downwards (Braitenberg and Schüz 1998, cf. Section 1.2), combining exclusively vertically aligned axons with the simplified axonal and dendritic morphological profiles would result in a “vertically staggered

random axonal
orientation yields
relevant
connectivity

connectivity" - neurons could then only project to targets located below them. It is in fact not a vertical alignment of axon orientation, but the anisotropy in neural connectivity - the observation of neuronal targets aligning with the axonal projection - that we try to capture and analyze in this model.

We will refer to the model as the *anisotropic geometric network model*. Trying to provide a simple, abstract model isolating anisotropy in connectivity, in most of this study the width $w(x)$ is assumed to be constant, $w(x) = w$, a notable exception being the exploration in ???. In the graph theoretic context the anisotropic network model is a random graph model, in which a realization of the random process results in a geometric directed graph with a special mode of connectivity. We can formally define such realization as:

Definition 1.1 (Anisotropic geometric graph). Let $n \in \mathbb{N}$ and $w \in (0, \infty)$. An *anisotropic geometric graph* $G_{n,w}$ then consists of a tuple (G, Φ, a) , of a simple directed graph G with $|V(G)| = n$ vertices and the maps $\Phi : V(G) \rightarrow [0, 1]^2$ and $a : V(G) \rightarrow [0, 2\pi)$, such that for every vertex pair $v, v' \in V(G)$ and edge $e \in E(G)$ with $s(e) = v$ and $t(e) = v'$ exists if and only if the inequalities

$$R_{-a(v)} (\Phi(v') - \Phi(v)) \hat{e}_x \geq 0 \quad \text{and} \quad \left| R_{-a(v)} (\Phi(v') - \Phi(v)) \hat{e}_y \right| \leq \frac{w}{2}$$

hold. Here R_φ is the rotation matrix of angle φ in the Cartesian plane and \hat{e}_x, \hat{e}_y are the standard unit vectors.

The anisotropic random graph model then is then giving the probability distribution over the set of anisotropic random graphs by describing a random process generating such graph.

Definition 1.2 (Anisotropic random graph model). Let $n \in \mathbb{N}$ and $w > 0$. The *anisotropic random graph model* $G(n, w)$ is a probability space over the set of anisotropic geometric graphs with a probability distribution induced by the following process: Let G be an empty graph with n vertices. Assign randomly and uniformly to every vertex $v \in V(G)$ a position $\Phi(v) \in [0, 1]^2$ and axonal orientation $0 \leq a(v) < 2\pi$. Then add edges such that (G, Φ, a) is an anisotropic geometric graph $G_{n,w}$.

*anisotropic model
is scale-free*

As with every geometric graph model introduced, we restrict the surface to be the unit square. This does not limit the model, as only the relative width of the axon band in regard to the surface's side length is determining connectivity statistics - the expected number of connections is easily obtained by the quotient of the area covered by the axon and the surface area, making connectivity statistics in the anisotropic random graph model scale-free.

The following maybe interpreted as a study of anisotropic geometric graphs in the light of a neuroscientific context. To enable such an analysis, a few more concepts are needed. The introduction of those concepts composes the rest of the chapter. A first important step is the numerical implementation of the anisotropic network model.

1.4 NUMERICAL IMPLEMENTATION

Numerical implementation of the anisotropic random graph model was achieved in Python¹. Relying on NumPy as part of the scientific Python library SciPy² for the more complex mathematical computations, the implementation also uses graph-tool³, to ensure convenient and efficient handling of the created networks.

The algorithm for the generation of anisotropic networks closely resembles Definition 1.1. After randomly distributing N neurons on the square of side-length s , for every neuron a random axon orientation $a \in [0, 2\pi)$ is chosen and an affine transformation, such that the current neuron is located at the origin and its axon projection aligns with the positive x-axis, secures a straightforward implementation of connectivity, using the the inequalities in Definition 1.1 as a rule for establishing connections.

To harness the numerical implemenation to generate networks, a set of parameters needs to be chosen. The network size N strongly influences the needed computational efforts in calculations based on the generated graphs and has thus been set to $N = 1000$. Choosing the surface side-length arbitrarily as $s = 100$, the axon width w determines connectivity in the network, the relation between width w and overall connection probability p being shown in Figure 1.7. In their analysis of connectivity of thick-tufted layer V pyramidal cells in neonatal rats (day 14), Song et al. (2005) report an overall connection probability of $p = 0.116$, consistent with prior reports of a cortical connection probability of $p \approx 0.1$. Choosing w to be constant, we determine the axon width such that overall connectivity matches the value report by Song et al. and obtain $w/2 = 12.6$ (Figure 1.7).

*parameter set
chosen to resemble
cortical circuits*

Having determined a suitable set of parameters as $N = 1000$, $s = 100$ and $w = 25.2$, we generate 25 graphs with this parameter set

¹ Python Software Foundation. Python Language Reference, version 2.7. Available at <http://www.python.org>

² Eric Jones, Travis Oliphant, Pearu Peterson and others. NumPy version 1.6.1. Available at <http://www.scipy.org>

³ Tiago P. Peixoto. Efficient network analysis. Version 2.2.18. Available at <http://graph-tool.skewed.de/>

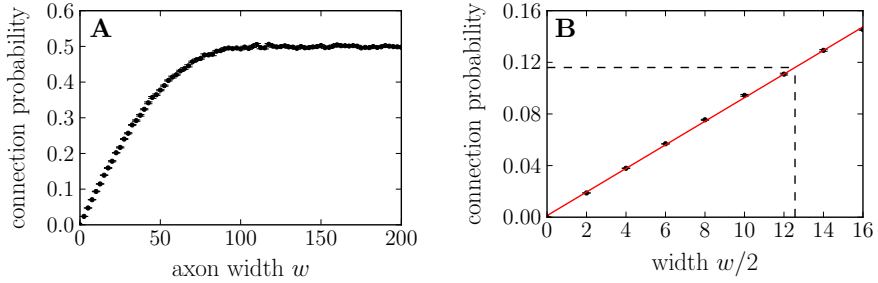


Figure 1.7: Axon width dependent connection probability determines parameter for numerical analysis Generating anisotropic networks with different axon widths w and extracting probability p of directed connection between two random nodes, demonstrates the dependency of p on the width parameter w . **A)** At an axon width of over $w = 100$, exceeding the square's side length, the connection probability saturates at $p = 0.5$, as axon bands are essentially “cutting” the square in a connected and unconnected half (c5b64f3e). **B)** For small w the connection probability is a linear function of w , allowing the width $w_S/2$ at which $p(w_S) = 0.116$ to be determined by a linear fit as $w_S/2 = 12.6$ (585a946f).

sample graphs as
reference for
structural analysis

(label: N1000w_ax126-flat_graph0-24). This set of sample graphs will serve as a reference for the following structural analysis. Extending the set by the (partially) rewired sample graphs (see Section 1.6) and by purely distance-dependent graphs best resembling the anisotropic networks (see Section 1.5) we obtain a resourceful reference for the analysis of structural features of anisotropic geometric graphs, that we will frequently employ to obtain quantitative and qualitative results.

1.5 DISTANCE DEPENDENT CONNECTIVITY

random graph
models in
Section ??

In Gilbert’s random graph model $G(n, p)$, probability of connection p is independently chosen and a fixed value for all vertex pairs. The anisotropic geometric graph model introduced in Section 1.3 is itself a random graph model - node positions as well as preferred directions of connection are uniformly at random distributed. In contrast to Gilbert’s model however, neither is the probability of connection between a given vertex pair independent of the realization of other edges in the graph, nor is it a fixed value - probabilities strongly depend on internode distance in the anisotropic geometric graph model introduced.

Analyzing dependencies in the anisotropic model, specifically by identifying prevalent patterns of connectivity and relating these modes of non-randomness to biological findings, is the main focus of Chapter ?? . However, such structural correlations may not necessarily be an inher-

ent feature of the network's anisotropy - distance dependent connectivity alone, as imposed by the model's specific geometry, may be the cause for emerging dependencies. It is therefore a crucial initial task to map the anisotropic model's distance dependent connection probability. Inferring connection probability as a function of internode distance and comparing it with computational results, in this section we explore distance connectivity of the anisotropic network model, securing a vital component in the analysis of structural features.

Theorem 1.3. *Let (G, Φ, a) represent an arbitrary realization of the anisotropic random graph model $G(n, w)$. Define $C : [0, \sqrt{2}] \rightarrow [0, 1]$ as the distance-dependent connection probability profile of (G, Φ) , that is such that $C(x)$ is the probability that for a vertex pair $(v, v') \in V(G)^2 \setminus \Delta_{V(G)}$ in distance $x = \|\Phi(v) - \Phi(v')\|$ the vertex v projects to vertex v' . Then*

$$C(x) = \begin{cases} \frac{1}{2} & \text{for } x \leq w/2 \\ \frac{1}{\pi} \arcsin\left(\frac{w}{2x}\right) & \text{for } x > w/2. \end{cases}$$

Proof. Let v, v' be a pair of vertices in $V(G)^2 \setminus \Delta_{V(G)}$ in Euclidean distance x of each other. The vector difference $\Phi(v') - \Phi(v)$ may then be written as $xe^{i\theta}$, with $0 \leq \theta < 2\pi$. We have

$$R_{-\alpha(v)}xe^{i\theta} = xe^{i(\theta - \alpha(v))}.$$

Only for suitable combination of θ and $\alpha(v)$ an edge from v to v' exists. Assuming $\alpha(v)$ fixed, we calculate the probability of connection depending on the random choice of θ . We can assume $\alpha(v) = 0$, otherwise the same argument holds for $\theta' = \theta - \alpha(v)$.

From 1.1 we obtain the necessary and sufficient conditions

$$x \cos \theta \geq 0 \quad \text{and} \quad |x \sin \theta| \leq \frac{w}{2}.$$

Choosing uniformly at random θ in the range of $[0, 2\pi)$, the first condition is satisfied with a probability of $\frac{1}{2}$. Consider for the second condition $\theta \in [0, \pi)$. We have

$$\sin \theta \leq \frac{w}{2x},$$

and for $x \leq \frac{w}{2}$ the inequality holds for all θ by definition of $\sin \theta$. In the case of $x > \frac{w}{2}$, we note that for the first condition to hold θ must already be in $[0, \frac{\pi}{2})$ and can thus write the second condition θ as

$$\theta \leq \arcsin \frac{w}{2x},$$

yielding $C(x)$ by combining the considerations above and using the symmetry of sine for θ in the third and fourth quadrant. \square

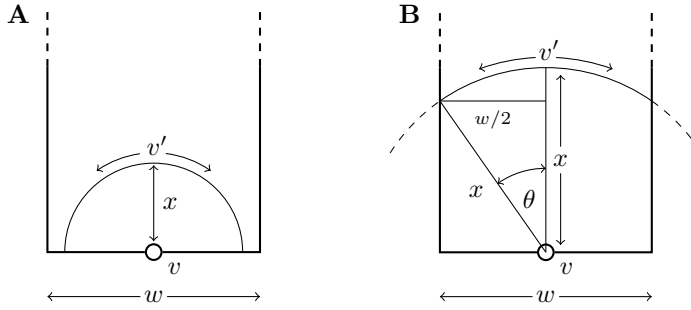


Figure 1.8: Illustrating the proof of Theorem 1.3 Distance-dependent connectivity profile $C(x)$ in an anisotropic geometric graph calculated from geometric dependencies. **A)** In the case of $x \leq w/2$, target v' may be located anywhere on the shown semicircle and therefore receives input from v with probability $1/2$. **B)** For $x > w/2$, suitable positions for target v' are dependent on x . The geometric relation $\sin \theta = w/2x$ leads to the distance-dependent connectivity profile as described in Theorem 1.3.

distance-dependent sample graphs as reference

We can verify this result by extracting the distance-dependent connection probabilities in the sample graphs created in Section 1.4. Combining data of all 25 graphs, we find that connection probabilities perfectly match the theoretical prediction (Figure 1.9). Additionally we're able to extend the reference sample graphs by distance-dependent networks (Definition ??). Using Theorem 1.3 in conjunction with the sample graph parameter set ($N = 1000$, $s = 100^4$, $w = 25.2$) we easily obtain the expected distance-dependent connectivity profile for the created sample graphs and, using this profile, generate purely distance-dependent networks⁵. Being highly interested in structural features not explained by distance-dependent connectivity, the numerical analysis in this work will heavily rely on these networks to identify aspects that are inherent to the anisotropy in connectivity.

⁴ The generalization of Theorem 1.3 to allow for arbitrary side-length s is trivial and omitted here

⁵ label: N1000-dist_depend-flat_graph-00-24.xml.gz

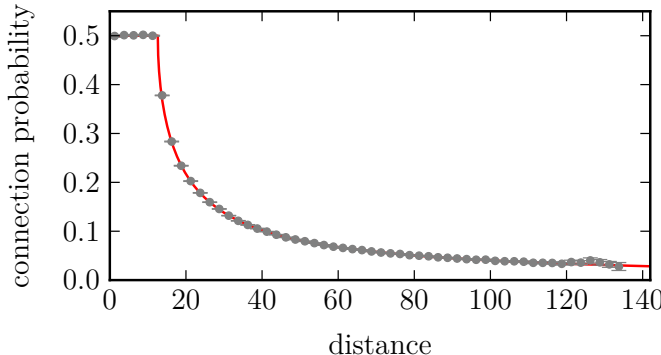


Figure 1.9: Predicted distance-dependent connection probability profile is matched by numerical results Averaging distance-dependent connection probabilities over the 25 sample graphs, we find the expected profile calculated in Theorem 1.3 is matched perfectly by the numerical results. (dbffa88e)

1.6 REWIRING

Distance-dependency as identified in the last section may already account for many of the structural features present in anisotropic networks. A central question of this study is: What structural aspects in the network are truly features of the anisotropy in connectivity? Although a quantitative measure for anisotropy will only be introduced in the next section, already here we are able to qualitatively observe the strong directionality in connectivity - edges originating from one node “point in the same direction”, effectively aligning with the orientation of the axonal projection of the source node (cf. Figure 1.6). To answer the question above, we need to introduce a method that eliminates this directionality, making networks essentially isotropic in connectivity. Then, structural features present in the original anisotropic networks, but not in their rewired, isotropic counterparts may be attributed to anisotropy.

eliminate
anisotropy to find
structures caused
by it

Rewiring as introduced here, provides the transition from anisotropic connectivity to networks isotropic in connectivity, closely resembling purely distance-dependent networks. Applying this process only partially then allows us to analyse structural features as they change with a varying degree of isotropy, asserting the importance of this process to our study. In designing the specific rewiring algorithm we identify two requirements that our implementation should satisfy:

1. elimination of anisotropy in connectivity
2. preservation of distance-dependent connectivity

The second point is especially important to us, as we want to impose isotropy on the network at “minimal cost”, that is by changing as little as possible about the other characteristics of the network’s connectivity. The following process respects both of the points above:

For every edge between vertices v and v' with inter-vertex distance x , identify neurons with distance to v in the range of $(x - \varepsilon, x + \varepsilon)$ as potential new targets. Then pick at random one of these vertices (including v') as a new target for the current edge, if such an edge doesn’t already exist (Figure 1.10).

In the graph theoretic context we formally define a rewiring as follows:

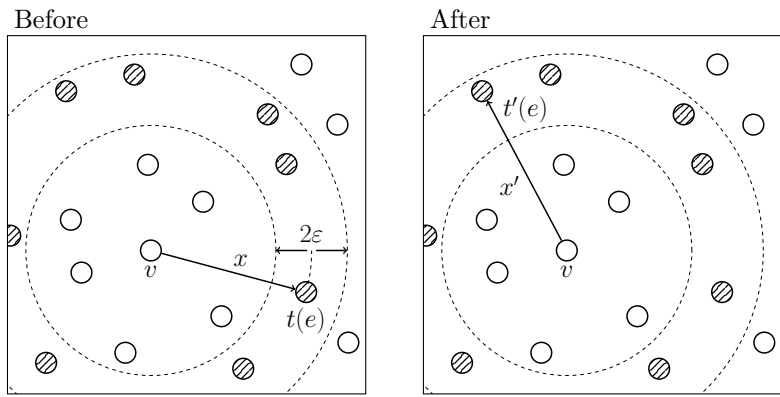


Figure 1.10: Rewiring transforms anisotropic geometric graphs to networks with isotropic connectivity For a given edge e with a distance x from its source vertex v to its target vertex $t(e)$, potential new targets (striped) are found in within a distance $(x - \varepsilon, x + \varepsilon)$ of v . The rewired edge then projects from v to a new target $t'(e)$, randomly chosen from the set of vertices within in this range. Inter-vertex distance between v and $t'(e)$ differs by less than ε from x , ensuring that for small ε the original distance-dependent connectivity is preserved. (Note that all targets within range are eligible for rewiring as no other edges exist. In general this is not the case.)

Definition 1.4. Let G be an anisotropic geometric graph with $|V(G)| = n$. Then we define a *rewiring* of G to be probability space over G_Φ^n , induced by the following process: For every edge $e \in E(G)$ uniformly at random pick a potential new target $t'(e)$ from the set $M_e = T_e \setminus K_e$, where T_e is the set of all vertices that differ in their distance to $s(e)$ less than ε from the distance of $s(e)$ to $t(e)$,

$$T_e = \{v \in V(G) \setminus s(e) \mid |d(s(e), v) - d(s(e), t(e))| < \varepsilon\}$$

and K_e the set vertices that already are connected to $s(e)$ by another rewired edge,

$$K_e = \{v \in V(G) \mid \exists e' \in E'(G) : s(e') = s(e), t(e') = v\},$$

where $E'(G)$ is the set of all edges that have been rewired already.

Note that in the way Definition 1.4 is formulated, it is possible for M_e to be empty for some edge e . In this case no new edge is realized and the resulting, rewired network has $|E(G)| - 1$ edges. In practice this happens negligibly seldom, out of approximately on average only 25.68 edges, with a standard deviation of 4.51 and accounting for roughly 0.02% of the rewired edges, are “lost” in this process (4afc2727).

We formulated Definition 1.4 in such a way, that distance-dependent connectivity is preserved. We verify this claim by the following estimation:

Let $\tilde{C}(x)$ be the distance-dependent connectivity profile of a rewiring R_ε of an anisotropic graph $G_{n,w}$. Denote with $C(x)$ the distance-dependent connection probability of the $G_{n,w}$. The expected value for $\tilde{C}(x)$ at any point x We estimate the expected difference between $\tilde{C}(x)$ and $C(x)$ at any point x as

$$\begin{aligned} \mathbf{E} [\tilde{C}(x) - C(x)] &= \int_{x-\varepsilon}^{x+\varepsilon} f(x') C(x') dx - C(x) \\ &= \frac{1}{2\varepsilon} \int_{x-\varepsilon}^{x+\varepsilon} C(x') - C(x) dx \\ &= \frac{1}{2\varepsilon} \left\{ \int_{x-\varepsilon}^x C(x') - C(x) dx - \int_x^{x+\varepsilon} C(x') - C(x) dx \right\} \\ &= \frac{1}{2\varepsilon} \end{aligned} \tag{1.1}$$

The rewiring margin ε thus simultaneously governs how many new targets are available for each edge and how well distance-dependency is preserved. Setting $\varepsilon = 1.25$ and applying the rewiring algorithm to the 25 sample graphs, we find that distance-dependent connectivity of the original graphs is matched (Figure 1.11) while at the same time ensuring that for any edge e sufficiently many new rewiring targets are available (??).

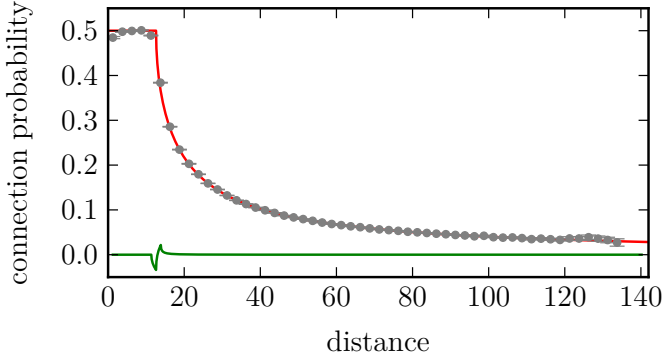


Figure 1.11: Rewiring with $\varepsilon = 1.25$ preserves distance-dependent profile in sample graphs Comparing the distance-dependent connection probabilities of the original graph (Theorem 1.3) in red with extracted of probabilities from the rewired ($\varepsilon = 1.25$) sample graphs in gray (errorbars SEM) we verify that distance-dependent connectivity is preserved when rewiring. The green curve shows the expected difference between the original and rewired distance profiles as estimated in Equation 1.1. (4f4dfcf1)

As a generalization of Definition 1.4, we define a partial rewiring $R_{\varepsilon,\eta}$, finding new targets only for a fraction η of all edges:

Definition 1.5. Let $\varepsilon > 0$ and $0 \leq \eta \leq 1$. A *partial rewiring* $R_{\varepsilon,\eta}$ of an anisotropic geometric graph $G_{n,w}$ is then a rewiring R_ε of $G_{n,w}$, in which every edge is rewired with a probability of η , otherwise it remains. To avoid the occurrence of multiple edges, K_e is then extended to include the targets of all edges originating from $s(e)$ that will not be rewired.

Clearly the result above of partial rewirings preserve distance-dependent connectivity. Using the we extend our set of sample graphs once more adding rewired graphs with rewiring margin $\varepsilon = 1.25$ with fractions $\eta = 0.25$, $\eta = 0.5$, $\eta = 0.75$ and $\eta = 1$, presenting a complete rewiring.

1.7 ANISOTROPY MEASURE

In the last section a method to rewire an anisotropic geometric graph, such that was introduced. From an . In this chapter we introduce.. capturing ..

The $G_{n,\Phi}$ be a geometric graph. Then, for every is the *preferred direction* and its length is

Mardia and Jupp (2000)

Figure 1.12: illustrate varying levels of anisotropy

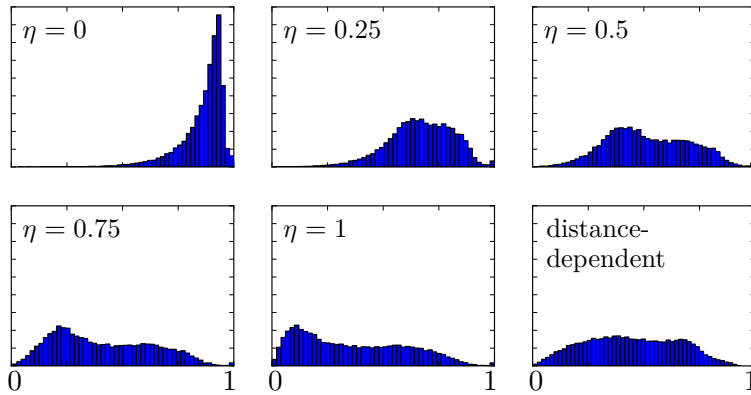


Figure 1.13: Rewiring significantly reduces anisotropy In data taken from the 25 sample graphs (Section 1.4), vertex isotropy degree distribution is shown for the original set of graphs ($\eta = 0$) The characteristic highly anisotropic profile found in the original is already significantly reduced by partial rewiring; anisotropy degree distribution in the fully rewired graphs resemble degree distribution of equivalent purely distance-dependent networks.

... suggesting that fully rewired anisotropic networks do not . There is however one difference in out-degree as an artifact of boundary confinement (Section ??).

1.8 SUMMARY AND DISCUSSION